Study of the Dzyaloshinskii-Moriya Interaction in Magnetic Tunnel Junction-Based Molecular Spintronic Devices with Antiferromagnetic-Ferromagnetic Electrodes

Babu Ram Sankhi, Christopher D'Angelo, Pawan Tyagi

Center for Nanotechnology Research and Education, Mechanical Engineering, University of District of Columbia, Washington, DC 20008, USA

***Abstract*- Magnetic tunnel junction-based molecular spintronic devices (MTJMSDs) hold promises for the creation of novel magnetic metamaterials. By coupling molecules with magnetic electrodes, MTJMSDs can exhibit unique magnetic properties and enable new magnetic phenomena. Understanding the interactions between molecules and electrode materials is essential for optimizing device performance. This paper presents a Monte Carlo Simulation (MCS) study of MTJMSDs, focusing on the impact of the Dzyaloshinskii-Moriya interaction (DMI). In the proposed system, a molecule is positioned between ferromagnetic (FM) and antiferromagnetic (AFM) electrodes. The DMI strength of the individual electrodes is varied independently to probe its impact on the magnetic properties of the electrodes and the overall MTJMSD. The simulations reveal that the FM electrode loses its magnetization entirely at the highest DMI values, consistent with our previous experimental observations where one of the FM electrode's magnetic identities disappeared following molecular treatment. Additionally, the magnetic moments of molecules decreased from 11 to 1 a.u. as the DMI increased in the FM electrode. The DMI-induced peculiar magnetic contrasts in the form of band structures are also investigated on both electrodes. This study highlights the significance of antisymmetric interactions, such as DMI, in determining the behavior of MTJMSDs and provides insights into how these interactions influence device properties across different magnetic phases.**

***Index Terms*—Antiferromagnets, DMI, MTJMSD, Spintronics.**

I. Introduction

Over the past decade, electron spin has emerged as a transformative factor in the semiconductor industry, giving rise to spintronics—a field that leverages both spin and charge properties of electrons to create new functionality in electronic devices [1]. Spintronics has revolutionized areas such as logic circuits and memory technologies, offering promising avenues for high-performance computing with improved speed, efficiency, and storage density[2, 3]. However, unlocking the full potential of spintronics requires deeper exploration and innovation, particularly in overcoming challenges associated with traditional material limitations[4, 5].

One significant challenge in spintronics is the reliance on conventional inorganic materials, such as metals and semiconductors, primarily due to their high Curie temperatures and tunable magnetic properties[5]. While effective, these materials face miniaturization, heat dissipation, and scalability constraints, particularly as devices become smaller and denser. Molecular spintronics, which aims to integrate the unique properties of molecules, seeks to address these issues by providing a platform for creating devices with reduced size, lower power consumption, and improved thermal management[6].

An innovative approach within molecular spintronics is the design of magnetic tunnel junction-based molecular spintronic devices (MTJMSDs)[7, 8]. These devices involve connecting molecular channels across the insulating barrier of magnetic tunnel junctions (MTJs) along the exposed edges. This molecular linkage mediates spin-dependent electron transport, a key mechanism supporting the device's functionality. The molecular spin moment plays a crucial role in this process, as a stronger molecular moment enhances the coupling between the molecule and the magnetic electrode[9]. This enhanced coupling not only affects the transport[10] and tunneling magnetoresistance (TMR)[11] but also enables spin-filtering via the molecular junction[12]. These features make MTJMSDs highly interesting for developing efficient spintronic devices, leading to many experimental and theoretical studies on their unique magnetic properties[7, 8, 13-15].

Of particular interest is a notable experimental finding that revealed unique magnetic contrasts on ferromagnetic (FM) electrodes in MTJMSDs, where the magnetic coherence of one electrode was disrupted following the attachment of an octa-metallic molecular complex [16]. This fascinating phenomenon has prompted further simulation studies aimed at understanding the underlying interactions that could lead to such intriguing observations[13, 17]. For instance, our previous theoretical work demonstrated how the nature of electrode combinations[17] and anisotropies [13] influences the molecular-electrode coupling. It also highlighted the potential for achieving multistate magnetoresistance in MTJMSDs incorporating both ferromagnetic (FM) and antiferromagnetic (AFM) electrodes[17]. In this study, molecule spins are uniquely aligned with FM and AFM electrodes, further emphasizing the importance of AFM electrodes in the MTJMSD system.

To deepen our understanding of these phenomena, we employ Monte Carlo Simulations (MCS) to study the influence of Dzyaloshinskii-Moriya interaction (DMI) on MTJMSDs with an AFM and FM electrode configuration. DMI, an antisymmetric exchange interaction between neighboring spins in magnetic materials, is known for its ability to create unique spin textures, including chiral domain walls and skyrmions[18]. In our study, we systematically vary the DMI within individual electrodes independently and analyze its impact on the magnetic properties, molecular spin moments, and band structures of different magnetic phases.

II. Computational Methodology

We utilized Monte Carlo Simulation (MCS)[13, 17, 19]to investigate the effect of the Dzyaloshinskii-Moriya interaction (DMI) on the magnetic properties of a cross-junction-shaped magnetic tunnel junction-based molecular spintronic device (MTJMSD). The MTJMSD structure consists of an antiferromagnetic (AFM) electrode on the left and a ferromagnetic (FM) electrode on the right. The device configuration is 11 × 50 × 50 (width × height × length), with a 5 × 5 atomic square molecule positioned between the AFM and FM electrodes (Fig.2a). The molecule spans one atomic plane in thickness and extends 50 atoms along its length, as shown in Fig. 2 and 3.

The system's equilibrium state was achieved through iterations based on the following Hamiltonian[15] [7, 8]:

$$H = -J_A\left(\sum_{i\in A} \boldsymbol{S_i}.\boldsymbol{S_{i+1}}\right) - J_F\left(\sum_{i\in F} \boldsymbol{S_i}.\boldsymbol{S_{i+1}}\right) - J_{mA}\left(\sum_{i\in A, i+1\in mol} \boldsymbol{S_i}.\boldsymbol{S_{i+1}}\right) - J_{mF}\left(\sum_{i-1\in mol, i\in F} \boldsymbol{S_{i-1}}.\boldsymbol{S_i}\right) - \boldsymbol{D_A}.\left(\sum_{i\in A} \boldsymbol{S_i}\times\boldsymbol{S_{i+1}}\right) - \boldsymbol{D_F}.\left(\sum_{i\in F} \boldsymbol{S_i}\times\boldsymbol{S_{i+1}}\right) \quad (1)$$

Where S_i and S_{i+1} represent neighboring spins. J_A , J_F , J_{mA} and J_{mF} are the strengths of Heisenberg exchange interactions for the AFM electrode , FM electrode, molecule-AFM electrodes and molecule- FM electrodes respectively. the term D_A and D_F corresponds to the DMI vector for AFM and FM.

In the simulation, the interaction strengths of individual electrodes were set to ensure antiferromagnetic and ferromagnetic behavior, with J_A= -1 and J_F = 1. The molecule-AFM and molecule-FM interfacial interactions were assigned values of JmA=1 and JmF= -1, respectively. To eliminate any unwanted coupling between the electrodes, both the inter-electrode exchange interaction (J_{FA}) and the DMI between the two electrodes D_{FA} were set to zero. Throughout the simulation, the molecular spin state was pinned at a constant value of 1.

Each simulation was run for 300 million iterations to achieve equilibrium, as determined through the Metropolis algorithm based on a Markov process[8]. The Spins were allowed to rotate in spherical polar coordinates, ensuring the realistic modeling of magnetic interactions.

The thermal energy for simulation was set to be 0.1(kT=0.1; k=Botzmann constant). It is noteworthy that in a ferromagnetic material exchange, coupling strength and Curie temperature(Tc) are both intrinsic and interdependent properties [20]. The Curie temperature can be converted into thermal energy by multiplying it with the Boltzmann constant (k). Subsequently, one can estimate the magnitude of unitless interatomic exchange coupling strengths J_F=1 by creating an analogy with corresponding thermal energy associated with Curie temperature ($k*T_c$). In our prior experimental work, we mainly used NiFe and Cobalt ferromagnetic materials in the MTJMSD. The Tc for NiFe alloys range from ≈773K to 873 K (500 to 600 °C) range[20]. Hence, if unitless J_F=1 corresponds to thermal energies with units if materials are known. With this corrolary, kT=0.1 unitless correspond to 0.1*(500-600°C) which turn out to be 50-60°C temperature range. Further details can be found in the reference[8].

To explore the impact of DMI, we varied the DMI strength independently along the Y-direction for each electrode. The DMI strength for the AFM electrode D_A was varied from 0 to 1 in increments of 0.2, while keeping the DMI of the FM electrode (D_F) at 0. Similarly, D_F was varied in the same range with D_A fixed at 0.

At equilibrium, the magnetic moments of the left and right electrodes aligned to yield a maximum total moment of 1250. The molecular moment reached a value of 16 when all sublattice spins were aligned in a same specified direction. The total moment is the sum of contributions from both electrodes and the molecule.

III. RESULT AND DISCUSSION

Fig. 1 illustrates the impact of the Dzyaloshinskii-Moriya interaction (DMI) on the time evolution of magnetic moments as a function of iteration counts, highlighting the system's equilibrium state achieved through Monte Carlo Simulation (MCS). Panels 1a and 1b depict the variations in magnetic moments for the antiferromagnetic (AFM) electrode at DMI values of D_A = 0.2 and D_A=1, respectively. In both plots, the red data points indicate that the net magnetic moment of the AFM electrode consistently stabilizes at zero. This consistency suggests that the DMI strength does not sufficiently influence the AFM electrode's total magnetic moment, likely because it is too weak to disrupt the stable, robust coupling of oppositely aligned spins within the AFM system. However, the reorganization of spins due to DMI, which forms discrete magnetic phases resembling narrow strips, is detailed elsewhere in this paper.

In contrast, the magnetic moment of the ferromagnetic (FM) electrode stabilizes around 1200 at equilibrium. Notably, saturation for the FM electrode occurs after around 200 million iterations (blue data sets in Fig.1a) for D_A = 0.2, while for D_A =1, this saturation is achieved from the onset of iteration counts (red data sets in Fig.1b). This difference may stem from D_A influencing the interaction between the AFM electrode and the molecule, subsequently affecting the exchange interaction between the molecule and the FM electrode. We surmise that DMI effect observed in the AFM electrode appears to transmit through molecular channels to the FM electrode, facilitating a quicker stabilization of its magnetic moments.

Fig. 1c and 1d explore the time evolution of magnetic moments in response to variations in the DMI of the FM electrode (D_F). For smaller values of D_F=0.2 (shown in Fig. 1c), the magnetic moments of the ferromagnetic electrode settle around 150 after approximately 40 million iterations. This behavior suggests that DMI may induce phase changes in the magnetic moments of the electrode, especially near critical points in the simulation.

Conversely, at the highest value of D_A=1 (Fig. 1d), the magnetic moments of the FM electrode align with the zero moment of the AFM electrode, as the spins within the FM electrode are affected and align oppositely (Figs. 3d and 3f). We surmise that at elevated DMI values, the antisymmetric exchange interaction dominates over the symmetric exchange interaction, characterized by the intra-atomic spin symmetric exchange interaction J_F=1. Consequently, the total magnetic moment of the MTJMSD also reaches zero, as it represents the sum of the magnetic moments from the AFM electrode, FM electrode, and molecule, with the molecule contributing minimally as maximum moments being only 16.

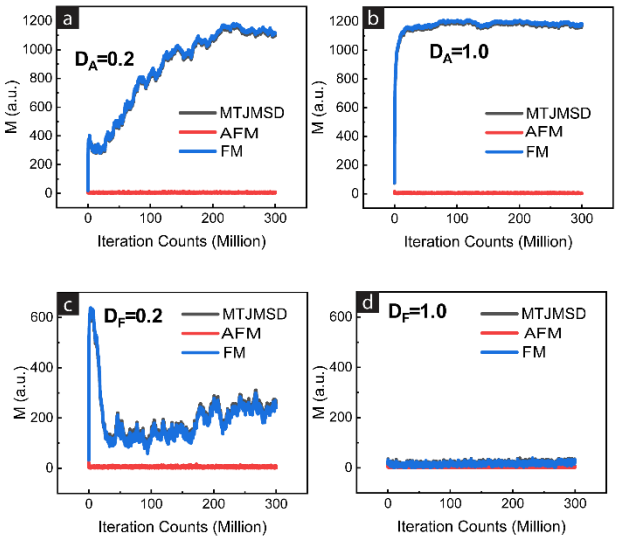

Fig.1. Temporal evolution of Magnetic moment as a function of the iteration counts at the end of simulations for: (a) Antiferromagnetic (AFM) electrode with DMI strength D_A=0.2 and D_F=0 (b) AFM electrode with D_A=1 and D_F=0 (c) ferromagnetic (FM) with D_F=0.2 and D_A=0 (d) FM electrode with DMI D_F=1, D_A=0. DMI is applied along y direction for all cases.

To gain deeper insights into the spin configurations of the AFM and FM electrodes within MTJMSD, we examined the equilibrium magnetic moments of the system's Heisenberg model on an atomic scale, as depicted in Fig. 2 and 3. In the 3D atomic model, the antiferromagnetic electrode is represented by vertical lattices, while the ferromagnetic electrode comprises horizontal lattices. The molecules are illustrated as small square lattices positioned between the two electrodes. The vertical color bars in Fig. 2 and 3 provide a normalized scale for the magnetic moments.

Monte Carlo simulations (MCS) were employed to address uncertainties by assigning random initial values to the variables in question. Each simulation run generates an output, and this process is repeated multiple times with varying inputs. Following energy minimization, the outcomes are averaged to yield an estimate. In the absence of DMI and anisotropies, the magnetic spins of the electrodes can align randomly in equilibrium state along any direction—x, y, or z—as demonstrated in our previous publications [7, 8] .

Fig. 2a-c and 2d-f illustrate the 3D lattice model of MTJMSDs, showcasing the magnetic spin orientations along the x, y, and z directions at equilibrium for D_A=0.2 and D_A=1, respectively. In this case, the DMI acted along the y-direction for the AFM electrode, that forced the alignment of spins to divide into two mutually perpendicular directions (i.e., x and z) as seen in Fig.2 (a,c,d and f). We surmise that this behavior arises because the antisymmetric DMI energy promotes orthogonal alignment between neighboring spins, contrasting with the parallel or antiparallel arrangement favored by the Heisenberg exchange interaction [21].

Conversely, the FM electrode did not have any applied DMI in Fig.2 i.e D_F=0, making its magnetic moment direction unpredictable at the end of MCS. For example, at D_A=0.2, the magnetic moment of the FM electrode is settled along the y-direction (Fig.2b), while, at D_A=1, it is aligned along the x-direction (Fig.2d). The color of the molecules is opposite to that of the FM electrode (Fig 2b) due to their antiferromagnetic coupling (J_{mF}=-1). In our simulation, while the left electrode is AFM with neighboring spins expected to align in opposite directions, the presence of DMI (D_A) causes the spins to rearrange themselves into stripes (Fig. 2a and 2c). Each band consists of antiferromagnetic domains separated by regions of null magnetization, indicated by green color, and these stripes maintain a nearly uniform width within the entire AFM electrode. As D_A increases to 1, the opposing magnetic phases within the stripes transition to narrower stripes (Fig. 2d and 2f). Notably, despite these changes in the nature of the stripes, the overall magnetic moment of the electrode remains zero, as quantified in Fig. 1a and Fig. 1b.

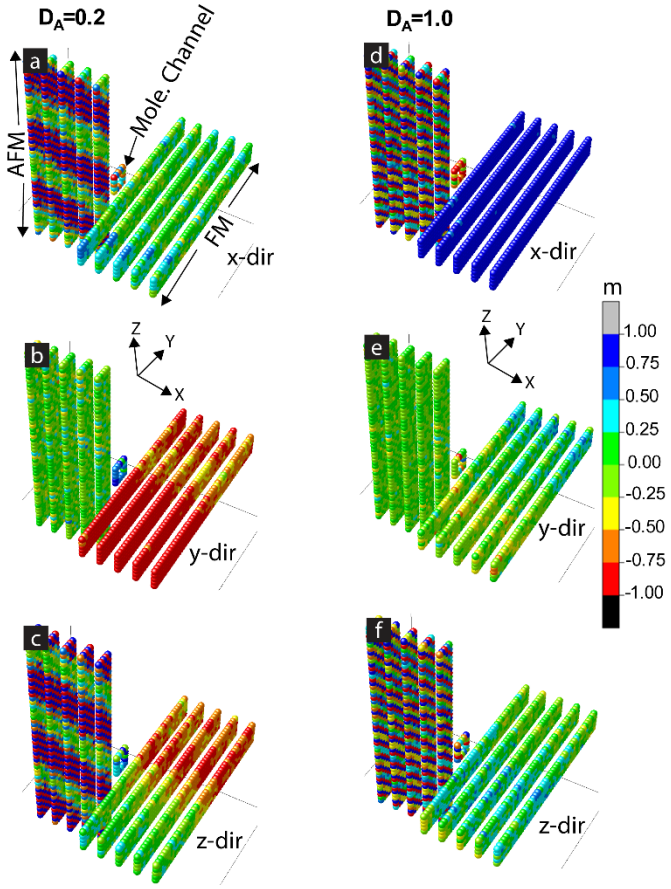

Fig.2. Three-dimensional lattice plots of the simulated MTJMSD comprising antiferromagnetic (AFM) on the left and ferromagnetic (FM) electrodes on the right and molecule channel in between them, For the AFM with DMI strength D_A=0.2: (a) spin orientation along the x-axis (b) spin orientation along y-axis and the (c) spin orientation along the z-axis. For D_A=1: (d) spin orientation along x-axis (e) spin orientation along the y-axis (f) spin direction along the z-axis. The color bar on the right indicates the strength and direction of the magnetic moment.

Fig. 3a–3c and 3d–3f illustrate the 3-D lattice models of the MTJMSD, with the DMI applied to the FM electrode (D_F)for values of D_F = 0.2 and 1.0, respectively. In the presence of DMI, the ferromagnetic electrode began to form magnetic domains of opposite phases, represented by blue and red colors in Fig. 3a and 3c. As the DMI strength increased, these magnetic domains also transitioned from broader to narrow stripes, as seen in Fig. 3d and 3f when D_F reached its maximum value of 1. Notably, the opposite magnetization phases within the entire electrode

led to a net magnetic moment of zero for the FM, as corroborated by the blue data points in Fig. 1d.

This behavior aligns with experimental findings in ferromagnet-based MTJMSDs, where unusual magnetization contrasts were observed, and one of the FM electrodes lost its magnetic coherent order following the treatment with paramagnetic octa-metallic molecular complexes (OMC)[22] [16] . Based on our simulations and the corresponding experimental results, we infer that these molecules can also exhibit antisymmetric exchange interactions with electrode spins, alongside Heisenberg exchange interactions through spin channels, as reported in previous studies [23, 24]. In these simulations Fig.3, the magnetic moments of FM settled along the x and z directions (Fig.3) due to the application of DMI in the y direction, while the magnetic moment of the AFM electrode consistently aligned along the y direction (Fig. 3b and 3e), remaining unaffected by the DMI on the FM electrode as applied (D_{FA}=0).

Interestingly, previous simulation publications revealed that the molecule was capable of transferring anisotropy-induced spin waves from one electrode to the other[7, 8]. Although we did not observe clear DMI-induced spin wave transfer through the spin channels, we anticipate that increasing the molecular size could enhance the clarity of spin transport between the electrodes. This intriguing possibility remains a topic for future exploration.

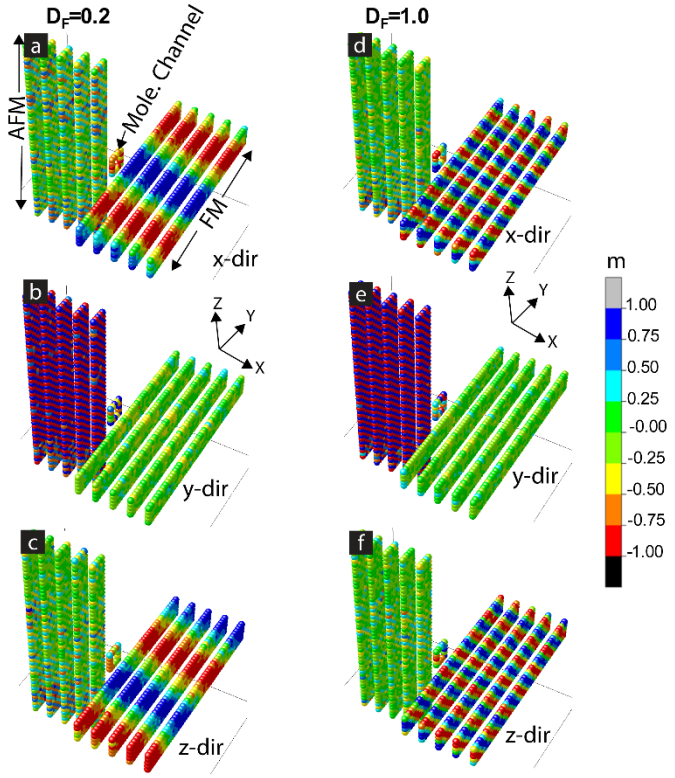

Fig.3. Three-dimensional lattice plots of the simulated MTJMSD. For the ferromagnetic electrode with DMI strength D_F=0.2: (a) spin orientation along the x-axis (b) spin orientation along y-axis and the (c) spin orientation along the z-axis. For D_F=1: (d) spin orientation along x-axis (e) spin orientation along the y-axis and (f) spin direction along the z-axis. The color bar on the right indicates the strength and direction of the magnetic moment.

We extracted the molecule's spin moment (M_{sm}) after the MTJMSD system reached an equilibrium state and plotted it as a function of DMI with and without the molecule (Fig. 4a). In the bare tunnel junction, the molecule's moments (blue and green data points of Fig.4a) remained constant at around 4, despite variations in the DMI across individual electrodes. This constancy is attributed to the random orientation of the molecule, resulting in a low net magnetic moment due to the absence of coupling with the electrodes.

When the molecule was incorporated into the MTJ system, acting as spin channels between the two electrodes, it coupled ferromagnetically with the AFM electrode (J_{mA}=1) and antiferromagnetically with the FM electrode (J_{mF}=-1). This coupling aligned more spins in a specific direction, enhancing M_{sm} to a peak value of ~11 (Fig. 4a) in the absence of DMI. However, the nature of M_{sm} variation was notably different for the AFM electrode's DMI (D_A) and the FM electrode's DMI (D_F). M_{sm} remained almost invariant (black data points) across all DMI values for the AFM. Conversely, it decreased to around 1 (red data points) for the highest value of FM DMI (D_F = 1). This reduction is linked to the increase in the number of magnetic stripes as the DMI value rises (Fig. 3d and 3f). With increasing DMI, the FM electrodes began to exhibit narrow bandwidths, and the molecule interacted with these narrow strips of distinct orientations (Fig. 3f).

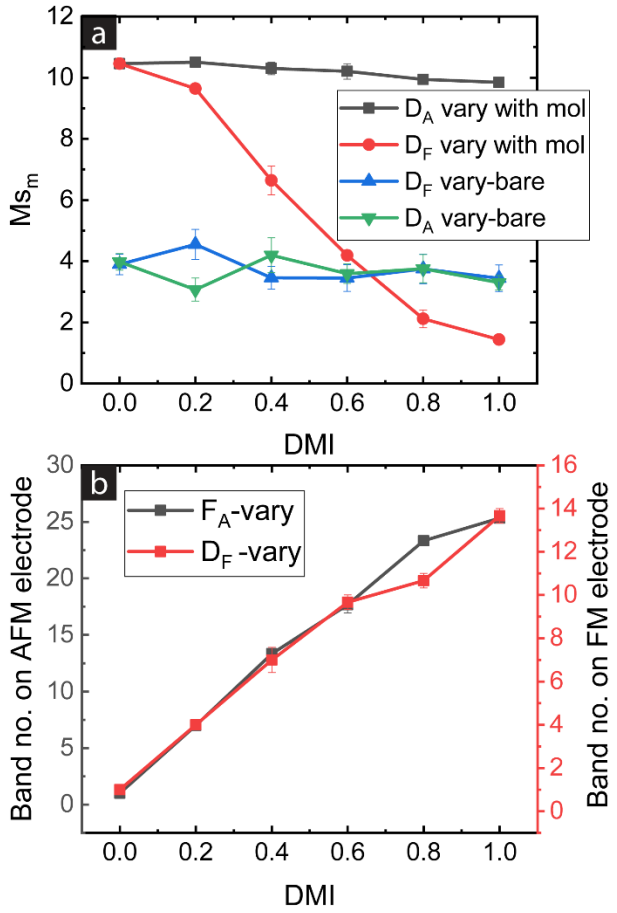

Fig 4. (a) Molecule's spin moments (Ms_m)as a function of DMI for Bare (green and blue data points) and molecule-treated (black and red data points) magnetic tunnel junction. (b) Dependence of band number on the AFM electrode (left axis) and FM electrode (right axis) on DMI. The notations D_F-vary and D_A-vary in the figure legend represent the variations of DMI strength for the antiferromagnetic electrode and the ferromagnetic electrodes respectively.

We also quantified the total number of stripes containing domains in the same phase (Fig. 4b). The trend of increasing band numbers in both electrodes remained consistent; however, the stripes numbers for the antiferromagnetic (AFM) electrodes were twice those of the ferromagnetic (FM) electrodes, reaching approximately 26 for AFM and 13 for FM. Such magnetic stripes could prove beneficial for data storage in logic devices.

IV. CONCLUSION

In our Monte Carlo simulation, we investigated the effect of the Dzyaloshinskii-Moria interaction (DMI) for the first time in a magnetic tunnel junction based molecular spintronics device (MTJMSD) comprising both antiferromagnetic and ferromagnetic electrodes. We systematically applied DMI magnitudes ranging from 0 to 1 in increments of 0.2 on each electrode to study its impact on the magnetic properties of each electrode and the entire MTJMSD system. Our results revealed that the ferromagnetic electrode formed stripes with oppositely aligned magnetic domains, resulting in a total magnetic moment of zero. This observation supports our previous experimental results, where molecule induced magnetic contrast and a loss of magnetization was noted in one of the FM electrode of the MTJMSD system. Furthermore, we analyzed the spin magnetic moment of the molecule across all DMI values and found a significant reduction from approximately 11 to 1 as the DMI approached 1 in FM electrode. This implies a substantial influence of DMI on the molecular spin interaction with the ferromagnetic electrodes, although minimal impact was observed on the molecule's spin due to changes in the DMI of the antiferromagnetic system. We quantified the number of stripes containing magnetic moments aligned in the same direction for the ferromagnetic electrode (13) and oppositely aligned moments for the antiferromagnetic electrode (26) at the highest DMI value. Our computational results for the MTJMSD provide valuable insights that not only support our previous experimental findings but also pave the way for future studies in selecting materials for magnetic tunnel junction-based molecular spintronics devices.

ACKNOWLEDGMENT

We acknowledg the funding sources: the National Science Foundation CREST Award, grant number HRD- 1914751, NSF-MRI grant 1920097, Department of Energy/ National Nuclear Security Agency (DE-FOA-0003945) and NASA MUREP Institutional Research Opportunity Grant under Cooperative Agreement #80NSSC19M0196.

REFERENCES

[1] S. D. Bader and S. S. P. Parkin, "Spintronics," *Annu. Rev. Condens. Matter Phys.,* vol. 1, no. 1, pp. 71-88, 2010.

[2] S. A. Wolf, J. Lu, M. R. Stan, E. Chen, and D. M. Treger, "The promise of nanomagnetics and spintronics for future logic and universal memory," *Proceedings of the IEEE,* vol. 98, no. 12, pp. 2155-2168, 2010.

[3] P. J. Rajput, S. U. Bhandari, and G. Wadhwa, "A review on—Spintronics an emerging technology," *Silicon,* vol. 14, no. 15, pp. 9195-9210, 2022.

[4] D. D. Awschalom and M. E. Flatté, "Challenges for semiconductor spintronics," *Nature physics,* vol. 3, no. 3, pp. 153-159, 2007.

[5] C. Felser, G. H. Fecher, and B. Balke, "Spintronics: a challenge for materials science and solid-state chemistry," *Angewandte Chemie International Edition,* vol. 46, no. 5, pp. 668-699, 2007.

[6] E. Coronado and M. Yamashita, "Molecular spintronics: the role of coordination chemistry," *Dalton Transactions,* vol. 45, no. 42, pp. 16553-16555, 2016.

[7] B. Dahal, M. Savadkoohi, E. Mutunga, C. D'Angelo, V. Lamberti, and P. Tyagi, "In-plane and out-of-plane anisotropies effect on Magnetic Tunnel Junction-Based Molecular Spintronics Device," *AIP advances,* 2022.

[8] P. K. Tyagi, C. Baker, and C. D'Angelo, "Paramagnetic molecule induced strong antiferromagnetic exchange coupling on a magnetic tunnel junction based molecular spintronics device," *Nanotechnology,* vol. 26, 2015.

[9] A. Grizzle, C. D'Angelo, J. Martínez-Lillo, and P. Tyagi, "Spin state of a single-molecule magnet (SMM) creating long-range ordering on ferromagnetic layers of a magnetic tunnel junction – a Monte Carlo study," *RSC Advances,* 10.1039/D1RA05473B vol. 11, no. 51, pp. 32275-32285, 2021, doi: 10.1039/D1RA05473B.

[10] P. Tyagi, D. F. Li, S. M. Holmes, and B. J. Hinds, "Molecular Electrodes At The Exposed Edge Of Metal/Insulator/Metal Trilayer Structures," *J. Am. Chem. Soc.,* vol. 129, no. 16, pp. 4929-4938, Apr 25

2007. [Online]. Available: <Go to ISI>://000245782800030.

[11] P. Tyagi and E. Friebe, "Large Resistance Change on Magnetic Tunnel Junction based Molecular Spintronics Devices," *J. Mag. Mag. Mat.,* vol. 453, pp. 186-192, 2018, doi: https://doi.org/10.1016/j.jmmm.2018.01.024.

[12] P. Tyagi, C. Riso, and E. Friebe, "Magnetic Tunnel Junction Based Molecular Spintronics Devices Exhibiting Current Suppression At Room Temperature," *Organic Electronics,* vol. 64, pp. 188-194, 2019.

[13] B. R. Dahal, M. Savadkoohi, A. Grizzle, C. D'Angelo, V. Lamberti, and P. Tyagi, "Easy axis anisotropy creating high contrast magnetic zones on magnetic tunnel junctions based molecular spintronics devices (MTJMSD)," *Scientific reports,* vol. 12, no. 1, p. 5721, 2022.

[14] M. Savadkoohi, D. Gopman, P. Suh, C. Rojas-Dotti, J. Martínez-Lillo, and P. Tyagi, "Spin Solar Cell Phenomenon on a Single-Molecule Magnet (SMM) Impacted CoFeB-Based Magnetic Tunnel Junctions," *ACS Applied Electronic Materials,* vol. 5, no. 6, pp. 3333-3339, 2023, doi: 10.1021/acsaelm.3c00369.

[15] A. Grizzle, C. D'Angelo, J. Martínez-Lillo, and P. Tyagi, "Spin state of a single-molecule magnet (SMM) creating long-range ordering on ferromagnetic layers of a magnetic tunnel junction–a Monte Carlo study," *RSC advances,* vol. 11, no. 51, pp. 32275-32285, 2021.

[16] P. Tyagi and C. Riso, "Magnetic force microscopy revealing long range molecule impact on magnetic tunnel junction based molecular spintronics devices," *Organic Electronics,* vol. 75, p. 105421, 2019/12/01/ 2019, doi: https://doi.org/10.1016/j.orgel.2019.105421.

[17] E. Mutunga, C. D'Angelo, and P. Tyagi, "Magnetic molecules lose identity when connected to different combinations of magnetic metal electrodes in MTJ-based molecular spintronics devices (MTJMSD)," *Scientific Reports,* vol. 13, no. 1, p. 16201, 2023/09/27 2023, doi: 10.1038/s41598-023-42731-9.

[18] I. Dzyaloshinsky, "A thermodynamic theory of "weak" ferromagnetism of antiferromagnetics," *Journal of physics and chemistry of solids,* vol. 4, no. 4, pp. 241-255, 1958.

[19] P. Tyagi, C. Riso, U. Amir, C. Rojas-Dotti, and J. Martínez-Lillo, "Exploring room-temperature transport of single-molecule magnet-based molecular spintronics devices using the magnetic tunnel junction as a device platform," *RSC Advances,* vol. 10, no. 22, pp. 13006-13015, 2020.

[20] J. M. Coey, *Magnetism and magnetic materials*. Cambridge University Press, 2010.

[21] L. Sandratskii, "Insight into the Dzyaloshinskii-Moriya interaction through first-principles study of chiral magnetic structures," *Physical Review B,* vol. 96, no. 2, p. 024450, 2017.

[22] D. Li *et al.*, "An S= 6 cyanide-bridged octanuclear FeIII4NiII4 complex that exhibits slow relaxation of the magnetization," *Journal of the American Chemical Society,* vol. 128, no. 13, pp. 4214-4215, 2006.

[23] M. Savadkoohi, B. R. Dahal, A. Grizzle, C. D'Angelo, and P. Tyagi, "Interaction between magnetic molecules and two ferromagnetic electrodes of a magnetic tunnel junction (MTJ)," *Journal of Magnetism and Magnetic Materials,* vol. 529, p. 167902, 2021.

[24] E. Mutunga, C. D'Angelo, A. Grizzle, V. Lamberti, and P. Tyagi, "Dramatic effect of electrode type on tunnel junction based molecular spintronic devices," *Organic Electronics,* vol. 106, p. 106526, 2022/07/01/ 2022, doi:

https://doi.org/10.1016/j.orgel.2022.106526.